Ji *et al. Microbial Cell Factories* (2025) 24:33
https://doi.org/10.1186/s12934-025-02663-7

Microbial Cell Factories

RESEARCH Open Access

Response mechanism of ethanol-tolerant *Saccharomyces cerevisiae* strain ES-42 to increased ethanol during continuous ethanol fermentation

Xue-Xue Ji[1,2], Quan Zhang[3], Bai-Xue Yang[1,2], Qing-Ran Song[1], Zhao-Yong Sun[1], Cai-Yun Xie[1,4*] and Yue-Qin Tang[1,2]

Abstract

Background Continuous fermentation offers advantages in improving production efficiency and reducing costs, making it highly competitive for industrial ethanol production. A key requirement for *Saccharomyces cerevisiae* strains used in this process is their tolerance to high ethanol concentrations, which enables them to adapt to continuous fermentation conditions. To explore how yeast cells respond to varying levels of ethanol stress during fermentation, a two-month continuous fermentation was conducted. Cells were collected at different ethanol concentrations (from 60 g/L to 100 g/L) for comparative transcriptomic analysis.

Results During continuous fermentation, as ethanol concentration increased, the expression of genes associated with cytoplasmic ribosomes, translation, and fatty acid biosynthesis progressively declined, while the expression of genes related to heat shock proteins (HSPs) and ubiquitin-mediated protein degradation gradually increased. Besides, cells exhibited distinct responses to varying ethanol concentrations. At lower ethanol concentrations (nearly 70 g/L), genes involved in mitochondrial ribosomes, oxidative phosphorylation, the tricarboxylic acid (TCA) cycle, antioxidant enzymes, ergosterol synthesis, and glycerol biosynthesis were specifically upregulated compared to those at 60 g/L. This suggests that cells enhanced respiratory energy production, ROS scavenging capacity, and the synthesis of ergosterol and glycerol to counteract stress. At relatively higher ethanol concentrations (nearly 80 g/L), genes involved in respiration and ergosterol synthesis were inhibited, while those associated with glycolysis and glycerol biosynthesis were notably upregulated. This suggests a metabolic shift from respiration towards enhanced glycerol synthesis. Interestingly, the longevity-regulating pathway seemed to play a pivotal role in mediating the cellular adaptations to different ethanol concentrations. Upon reaching an ethanol concentration of 100 g/L, the aforementioned metabolic activities were largely inhibited. Cells primarily focused on enhancing the clearance of denatured proteins to preserve cellular viability.

Conclusions This study elucidated the mechanisms by which an ethanol-tolerant *S. cerevisiae* strain adapts to increasing ethanol concentrations during continuous fermentation. The findings suggest that the longevity-regulating pathway may play a critical role in adapting to varying ethanol stress by regulating mitochondrial

*Correspondence:
Cai-Yun Xie
xiecy@scu.edu.cn

Full list of author information is available at the end of the article

respiration, glycerol synthesis, ergosterol synthesis, antioxidant enzyme, and HSPs. This work provides a novel and valuable understanding of the mechanisms that govern ethanol tolerance during continuous fermentation.

Keywords *Saccharomyces cerevisiae*, Continuous ethanol fermentation, Dynamic response mechanism, Ethanol stress, Comparative transcriptome

Background

Continuous fermentation is a key technology in the industrial production of bioethanol, as it helps to increase productivity, minimize non-productive downtime, and reduce overall production costs [1, 2]. However, the fermenting microorganisms are continuously exposed to high ethanol concentrations. Ethanol has adverse effects on cells, such as inhibiting cell growth and viability, limiting fermentation productivity, and reducing ethanol yield [3]. The inhibitory effect of accumulated ethanol on ethanol-producing microorganisms is one of the key challenges affecting the performance of the fermentation system [4]. To achieve high ethanol titer and productivity, industrial production typically employs multistage systems or tanks-in-series systems, combined with cell recycling or cell immobilization techniques [1, 5–8]. However, the use of multiple fermentation tanks and cell recycling or immobilization techniques increases production costs. To further reduce production costs and improve fermentation efficiency, enhancing microbial ethanol tolerance is crucial.

Saccharomyces cerevisiae is an ideal species for large-scale bioethanol fermentation due to its good tolerance to high osmotic pressure and high ethanol concentrations [9]. Although *S. cerevisiae* can tolerate up to 120 g/L of ethanol, a concentration of around 40 g/L can cause 50% growth inhibition, thereby limiting ethanol production [10, 11]. A deep understanding of the toxic effects of ethanol on yeast cells and the response mechanisms of yeast cells to ethanol can provide guidance for improving ethanol tolerance. Studies have shown that ethanol interferes with cell membrane structure, protein homeostasis, energy status, and the cell cycle [3, 10, 12]. Accordingly, yeast cells develop several tolerance mechanisms, such as adjusting the cell membrane composition, inducing the H^+-ATPase pump, enhancing antioxidant resistance, strengthening energy supply, synthesizing protective substances, inducing heat shock proteins (HSPs), and maintaining redox balance [13, 14]. However, these conclusions are based on the response of cells to short-term ethanol stress in laboratory batch fermentations and do not accurately reflect the response of cells to long-term high ethanol stress during continuous fermentation. Exploring how yeast cells respond to persistent high ethanol stress can provide guidance for constructing ethanol-tolerant strains suitable for continuous ethanol fermentation.

Few studies have focused on the response mechanisms of *S. cerevisiae* during continuous ethanol fermentation [15, 16]. Li et al. analyzed the transcriptional differences in cells from the first, third, and fifth fermentors, which had ethanol concentrations of approximately 30, 60, and 80 g/L, respectively, in a continuous ethanol fermentation process using 11 serial fermentors [15]. Since the first two fermentors primarily support cell growth and supply cells to the later fermentors, it is difficult to accurately assess the impact of ethanol on cell growth and fermentation. Zhang et al. conducted very high gravity (VHG) continuous ethanol fermentation using a 2.5 L fermenter with 280 g/L glucose in the feed [16]. They observed a periodic oscillation in the levels of residual glucose, ethanol, and biomass over a period of approximately 150 h. Specifically, the ethanol concentration oscillated between 40 g/L and 70 g/L. The study primarily explored the mechanisms underlying the process oscillation. Therefore, further studies are needed to elucidate the response mechanisms of *S. cerevisiae* to the accumulating ethanol during continuous ethanol fermentation.

In this study, we established a one-stage continuous ethanol fermentation system using an ethanol-tolerant *S. cerevisiae* strain. Over a two-month fermentation period, the ethanol concentration in the fermenter was increased by gradually raising the feeding glucose concentration from 130 g/L to 260 g/L. Cells were collected at five different time points for comparative transcriptomic analysis. The aim of this research is to reveal the response mechanisms of ethanol-tolerant *S. cerevisiae* strain to increasing ethanol concentrations from 60 g/L to 100 g/L during continuous fermentation, thereby providing valuable information for the development of ethanol-tolerant strains.

Methods

Strains and medium

In our previous study, we developed a multiple stress-tolerant flocculating *S. cerevisiae* strain E-158, which has strong tolerance to high ethanol, high temperature, and high osmotic stress, through the following approach: Atmospheric and Room Temperature Plasma (ARTP) mutagenesis and four rounds of genome shuffling were applied to the parental strain KF7, generating a pool of mutant strains. The most ethanol-tolerant mutant C4-189, screened under 15% ethanol stress, and the most heat-tolerant mutant W3-9, screened at 44℃, were crossed to generate heterozygous diploids. From these,

the multi-stress tolerant strain E-158 was obtained [17]. A homozygous diploid strain, ES-42, which exhibits tolerance comparable to that of E-158, was obtained from E-158 through sporulation, spore isolation, and cultivation. In the present study, ES-42 was utilized for continuous fermentation.

The YP medium (10 g/L yeast extract and 20 g/L peptone) containing 20 g/L glucose (referred to as YPD20) was used for the routine cultivation of yeast cells. YP medium supplemented with 50 g/L glucose (YPD50) was used for pre-cultivation. YP media with various glucose concentrations were used throughout the continuous fermentation process: 130 g/L (YPD130), 200 g/L (YPD200), and 260 g/L (YPD260). Additionally, the NYPD260 medium, which contains 17 g/L yeast extract, 34 g/L peptone, and 260 g/L glucose, was also utilized in the continuous fermentation process.

One-stage continuous ethanol fermentation

The device was composed of three main components: a fermentation tank (MDL series, BE. MARUBISHI Co., Ltd, Japan), a feeding and discharging system, and an air pump. The fermentation tank had a total capacity of 1 L and a working volume of 0.6 L. Medium inflow and culture outflow were managed through peristaltic pumps, which controlled the dilution rate by adjusting their flow rates. Sterilized air was introduced uniformly from the bottom of the fermentation tank via a ventilation system, with its flow regulated by adjusting the gas flow meter. Previous studies have demonstrated the positive effect of aeration on cellular activity during continuous fermentation [18, 19]. Therefore, this study adopted a continuous micro-aeration strategy in the one-stage fermentation process to achieve higher ethanol concentrations.

Yeast cells were activated on a YPD20 agar plate and then inoculated into a 500 mL Erlenmeyer flask containing 100 mL of YPD50 medium. The cells were cultivated at 30 °C and 160 rpm for 16 h. After this, cells from 60 mL of the culture broth were harvested by centrifugation. The collected cells were then inoculated into the fermentation tank containing 600 mL of YPD130 medium. The continuous fermentation process was conducted at 33 °C and 200 rpm. The fermentation process was divided into three distinct operational periods based on the glucose concentrations in the feed. For the first period, the inlet glucose concentration was set at 130 g/L. The dilution rate was maintained at 0.05 h^{-1}, while the aeration rate was progressively increased from 0.01 vvm to 0.05 vvm in order to enhance cellular activity. For the second period, the inlet glucose concentration was increased to 200 g/L. During this period, the dilution rate remained constant at 0.05 h^{-1}, and the aeration rate was gradually increased from 0.01 vvm to 0.07 vvm in order to enhance cellular activity. To further enhance the ethanol titer, the aeration rate was kept at 0.07 vvm, and the dilution rate was reduced from 0.05 h^{-1} to 0.025 h^{-1}. Reducing the dilution rate extended glucose retention time in the reactor, increasing glucose consumption and thereby boosting ethanol concentration. For the third period, the inlet glucose concentration was increased to 260 g/L, and the aeration rate was kept at 0.07 vvm. The dilution rate was kept at 0.025 h^{-1} for 7 days and then reduced to 0.0125 h^{-1} to increase the ethanol concentration. Finally, the nitrogen source content was increased to investigate its effect on ethanol production.

Analytical methods

Every 24 h, fermented broth was drawn from the fermentation tank and centrifuged at 10,000 rpm for 2 min. Due to the flocculating properties of ES-42, the cell pellet was resuspended in 0.1 M EDTA for effective deflocculation and dispersion. The cell suspension was then stained with a methylene blue solution (0.01 g/L) for 5 min before being used for counting with a hemocytometer. Dead cells appeared blue, whereas viable cells remained unstained.

Meanwhile, the supernatant was filtered through a 0.22 μm membrane filter and used for the measurement of glucose, ethanol, and glycerol concentrations as previously described [20]. Glucose and glycerol were determined by high-performance liquid chromatography (HPLC) equipped with a RID-20 A refractive index detector (Shimadzu, Japan) and an Aminex HPX-87 H column (Bio-Rad, USA). Ethanol was measured by gas chromatography (GC) equipped with a flame ionization detector (FID) and a TC-1 capillary column. Isopropanol was used as the internal standard.

RNA extraction and sequencing

Fermentation broth was collected at multiple time points during continuous fermentation, each corresponding to different ethanol concentrations. Three individual samples taken from the same point served as replicates. Following centrifugation at 5,000 rpm for 2 min, the cells were used for RNA extraction using the Yeast RNA Kit (Omega, USA). The quality and concentration of the total RNA were measured using a Nanodrop 2000 (Thermo Scientific, USA) and a 2100 Bioanalyzer (Agilent, USA). High-throughput RNA sequencing analysis was conducted using the Illumina Novaseq 6000 platform by Shanghai Majorbio Technology Co., Ltd. Approximately 6 GB of clean data per sample was used for conducting the transcriptional analysis. The raw sequence data are accessible via the SRA accession number PRJNA1114950.

Comparative transcriptomic analyses

After the sequencing data underwent quality control and statistical analysis, the remaining reads were

aligned to the *S. cerevisiae* S288C reference genome via the Hisat2 software. Gene expression levels were quantified in Transcripts per Million reads (TPM) through the RSEM software. To investigate the inter-sample relationship patterns, Principal Component Analysis (PCA) was conducted on the full gene expression profiles using the FactoMineR package in R. Weighted Gene Co-expression Network Analysis (WGCNA) was performed on 15 RNA samples using the WGCNA package in R [21, 22]. The analysis consists of three main parts. First, the data were preprocessed. Genes with TPM < 10 in over 90% of the samples and TPM = 0 in over 80% of the samples were removed. Gene expression data were then normalized using $\log_2(\mathrm{TPM}+1)$, and samples were clustered to exclude outliers. Second, the co-expression network was constructed. An appropriate soft threshold was chosen to create the topological overlap matrix (TOM). A correlation matrix was then established based on pairwise Pearson correlations among all genes. Hierarchical clustering was performed on the TOM matrix to identify gene modules with similar expression profiles, and the DynamicTreeCut algorithm was used to merge modules with comparable expression patterns. Third, the association between modules and traits was analyzed. PCA was performed on the gene expression matrix of each module, and the first principal component (identified as ME) was used to represent the module's expression pattern. The correlations between each module ME and the traits were calculated. Gene significance (GS) values, representing the correlation between each gene and the trait, and module membership (MM) values, representing the correlation between each gene and its module, were obtained. Genes with MM > 0.8 and GS > 0.2 in the interested modules were selected as potential key candidate genes for further analysis [22].

Key genes from modules of interest were subjected to Gene Ontology (GO) and Kyoto Encyclopedia of Genes and Genomes (KEGG) pathway enrichment analysis using Metascape [23]. GO terms and KEGG pathways with an adjusted *p* value (padj) < 0.05 were considered to be significantly enriched. To compare gene expression across different time points, the TPM values of the target genes were linearly normalized to scale the expression levels between 0 and 1 using the formula: $\mathrm{X} = \frac{x-\min(x)}{\max(x)-\min(x)}$

Results

Performance of continuous ethanol fermentation

The one-stage continuous fermentation process extended over 61 days, segmented into three distinct periods according to the inlet glucose concentration (Fig. 1). In the first period, the inlet glucose concentration was set at 130 g/L, with a dilution rate of 0.05 h^{-1}. The aeration rate was gradually increased from 0.01 vvm to 0.05 vvm over the course of 15 days, during which all glucose was consumed. Initially, the ethanol concentration was recorded at 55.7 g/L. As fermentation progressed, the ethanol concentration initially climbed to 60.0 g/L before dropping to 58.3 g/L. Meanwhile, the glycerol concentration decreased from approximately 2.3 g/L to about 1.8 g/L, with its yield relative to consumed glucose decreasing from 0.018 g/g to 0.014 g/g. Notably, enhancing the aeration rate from 0.025 vvm to 0.05 vvm led to a significant increase in the total and viable cell counts (Fig. 1b). This indicated that a slight increase in oxygen supply can markedly boost cell viability and activity during continuous fermentation.

The second period extended for 25 days, during which the inlet glucose concentration was set at 200 g/L. Initially, the dilution rate was kept constant at 0.05 h^{-1}, while the aeration rate was gradually increased from 0.01 vvm to 0.07 vvm. As a result, the ethanol concentration rose from 65.4 g/L to 73.7 g/L, with a concurrent reduction in residual glucose. Meanwhile, the glycerol concentration remained stable at approximately 3.5 g/L, though its yield decreased from 0.027 g/g to 0.021 g/g. These findings indicated that an adequate oxygen supply can significantly promote ethanol fermentation. Despite these improvements, it was noted that complete glucose consumption was not achieved within the average retention time of 20 h. To further elevate the ethanol concentration, the dilution rate was subsequently lowered to 0.025 h^{-1}. Consequently, the ethanol concentration reached approximately 86.9 g/L, while the residual glucose concentration dropped to around 12.1 g/L. Although the glycerol concentration remained stable, the yield further decreased to 0.019 g/g.

In the final period (spanning 21 days), the inlet glucose concentration was elevated to 260 g/L, while maintaining an aeration rate of 0.07 vvm. Initially, with a dilution rate of 0.025 h^{-1}, the ethanol concentration settled around 80 g/L, accompanied by a residual glucose concentration of about 70 g/L. These results suggested that high glucose concentration might have an inhibitory effect on ethanol fermentation to some extent. During this phase, the glycerol concentration was around 5.1 g/L, with a yield of 0.026 g/g. To further optimize ethanol production, the dilution rate was reduced to 0.0125 h^{-1}. This adjustment led to an increase in the ethanol concentration to 101.9 g/L, while the residual glucose concentration decreased to 30.3 g/L. Concurrently, the glycerol concentration rose to nearly 7.3 g/L, with its yield reaching 0.036 g/g. Further increasing the nitrogen source did not result in any increase in ethanol concentration. This indicated that nitrogen supply was not the primary factor influencing cell metabolism during this phase. Overall, compared to the first two periods, the third period

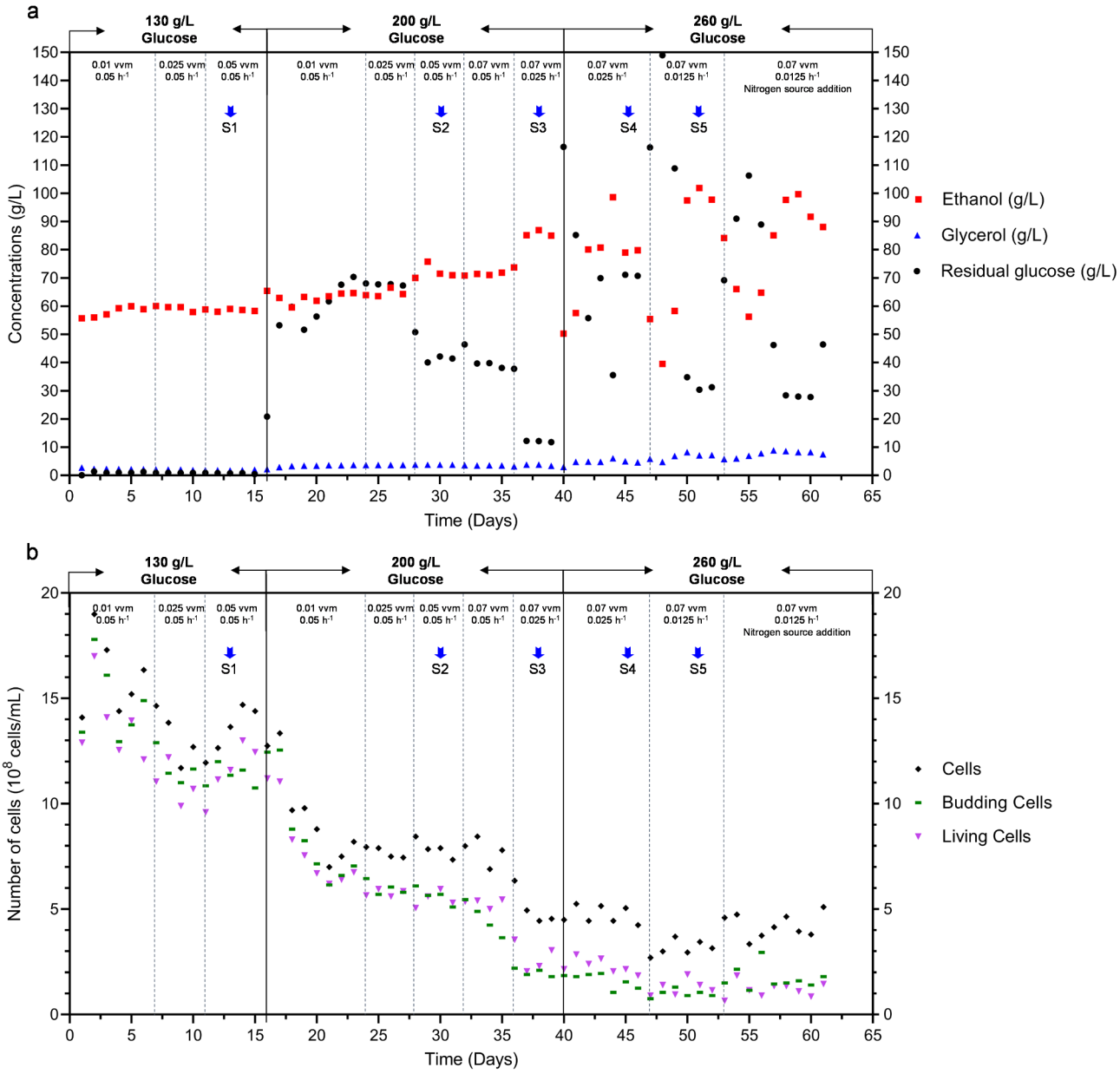

Fig. 1 Continuous ethanol fermentation of strain ES-42 under different glucose concentrations in the influent. (**a**) Ethanol, glycerol, and residual glucose concentrations. (**b**) Number of cells, budding cells, and living cells. S1, S2, S3, S4, and S5 denote the distinct time points at which RNA was extracted

showed significant fluctuations in both ethanol production and residual glucose levels. These fluctuations may be similar to the process oscillations commonly observed in continuous ethanol fermentation under VHG conditions, which are primarily caused by ethanol toxicity [4, 16].

Throughout the entire continuous fermentation process, a declining trend was observed in the numbers of total cells, living cells, and budding cells (Fig. 1b). During the first period, the number of live cells fluctuated between 9.6×10^8 cells/mL and 17×10^8 cells/mL. Upon entering the second period, the number of live cells gradually decreased from 11.2×10^8 cells/mL to 2.2×10^8 cells/mL. In the third period, the number of live cells further reduced from 2.8×10^8 cells/mL to approximately 1.2×10^8 cells/mL. Notably, as the ethanol concentration increased, both the survival rate and the budding rate of the cells showed a corresponding gradual decline (Fig. S1). These observations indicated that ethanol concentration plays a crucial role in influencing cell growth and viability.

Weighted co-expression network construction and key modules identification

To elucidate the response mechanism of ES-42 to increasing ethanol concentrations during continuous fermentation, RNA was extracted at five distinct time points (S1 to S5) for comparative transcriptomic analysis. The specific conditions were shown in Table 1. At S1, the inlet glucose concentration was 130 g/L and the ethanol concentration was 59 g/L. At S2, the inlet glucose concentration was 200 g/L and the ethanol concentration was 71.5 g/L. At S3, the inlet glucose concentration remained at 200 g/L, but the ethanol concentration increased to 86.9 g/L by reducing the dilution rate to 0.025 h^{-1}. At S4, the inlet glucose concentration was 260 g/L and the ethanol concentration was 79 g/L. At S5, the ethanol concentration increased to 101.9 g/L by reducing the dilution rate to 0.0125 h^{-1}. For each time point, three biological replicates were prepared, resulting in a total of 15 RNA samples. The PCA analysis results indicated that as the ethanol concentration increased, the differences among samples became more pronounced (Fig. S2).

We applied WGCNA to obtain a systemwide understanding of groups of genes whose co-expression patterns were highly correlated during continuous fermentation. After data filtering, 5826 genes were included in the WGCNA analysis. First, 15 samples were clustered to detect any potential outliers. The sample size was not confined by height, as the cutoff value was set at 120 (Fig. S3a). The "pickSoftThreshold" function was utilized to determine the optimal soft-power threshold. The scale-free topology fit index did not reach 0.8 (Fig. S3b) and the mean connectivity remained relatively high (Fig. S3c), which might be due to an intriguing biological variable. Therefore, the recommended default value of $\beta = 9$ was adopted. For the clustering segmentation, the minimum module size was set to 50, and the deepSplit parameter was adjusted to 2 (indicating a medium level of sensitivity). The hierarchical clustering dendrogram in Fig. 2a illustrated co-expressed genes with high correlation, while their relative expression levels were visualized through a heat map. Five distinct co-expression modules that exhibited diverse patterns of gene expression were identified. Notably, the blue module showed the most significant correlation with ethanol, and also showed a strong correlation with living cells (Fig. 2b). Therefore, the blue module, consisting of 2105 genes, was considered a key module for further investigation. To assess the relevance of each gene to the blue module and traits such as ethanol and living cells, the MM and GS values for each gene were calculated (Fig. 2c, Fig. S4). Applying the criteria of MM > 0.8 and GS > 0.2, 1756 genes within the blue module were identified as hub genes. These hub genes were considered pivotal to the function of the blue module.

Table 1 Phenotypic characteristics at the five time points for RNA extraction

	S1	S2	S3	S4	S5
Ethanol (g/L)	59.00	71.50	86.90	79.00	101.90
Inlet glucose (g/L)	130	200	200	260	260
Aeration rate (vvm)	0.05	0.05	0.07	0.07	0.07
Dilution rate (h^{-1})	0.05	0.05	0.025	0.025	0.0125
Residual glucose (g/L)	0.70	42.20	12.10	71.10	30.30
Glycerol (g/L)	1.80	3.69	3.78	4.97	7.11
Glycerol yield (g/g)	0.014	0.023	0.020	0.026	0.031
Days	12	30	38	45	51

vvm (air volume per culture volume per minute); The glycerol yield was calculated based on the amount of consumed glucose

A dynamic gene expression landscape during continuous fermentation

The 1756 key genes were subjected to GO and KEGG enrichment analysis. The results showed that 88 GO terms were significantly enriched (padj < 0.05), which could be grouped into 16 categories (Table S1, Fig. 3a). Simultaneously, 25 KEGG pathways were significantly enriched (padj < 0.05) (Table S2, Fig. 3b). These processes and pathways may reflect how yeast cells cope with ethanol stress during continuous fermentation. Genes involved in these processes and pathways were analyzed for their expression patterns and classified accordingly (Fig. 4). Specifically, genes related to cytoplasmic ribosomes, translation, V-type ATPase, and fatty acid biosynthesis consistently decreased. Genes involved in mitochondrial ribosomes, oxidative phosphorylation, the tricarboxylic acid (TCA) cycle, the pentose phosphate pathway (PPP), actin cytoskeleton, ergosterol synthesis, and antioxidant enzymes peaked at S2 and then gradually declined. Glycolysis-related genes increased, peaking at S4, and then sharply dropped. Notably, glycerol synthesis genes and longevity-regulating genes showed a bimodal pattern, with higher levels at S4. Additionally, genes encoding HSPs and those involved in ubiquitin-mediated degradation showed a rising trend throughout the fermentation. The following sections provide a detailed analysis.

Expression of genes associated with translation

Twenty terms were closely associated with translation, encompassing various aspects such as cytosolic ribosome, cytosolic small ribosomal subunit, sequence-specific mRNA binding, ribosome assembly, and translation reinitiation (Table S1). The enriched KEGG pathways also included ribosome and N-Glycan biosynthesis (Fig. 3b).

Almost all genes related to cytoplasmic ribosomes showed the highest expression levels at S1, after which their expression declined in correlation with increasing ethanol concentrations (Fig. S5). However, genes coding

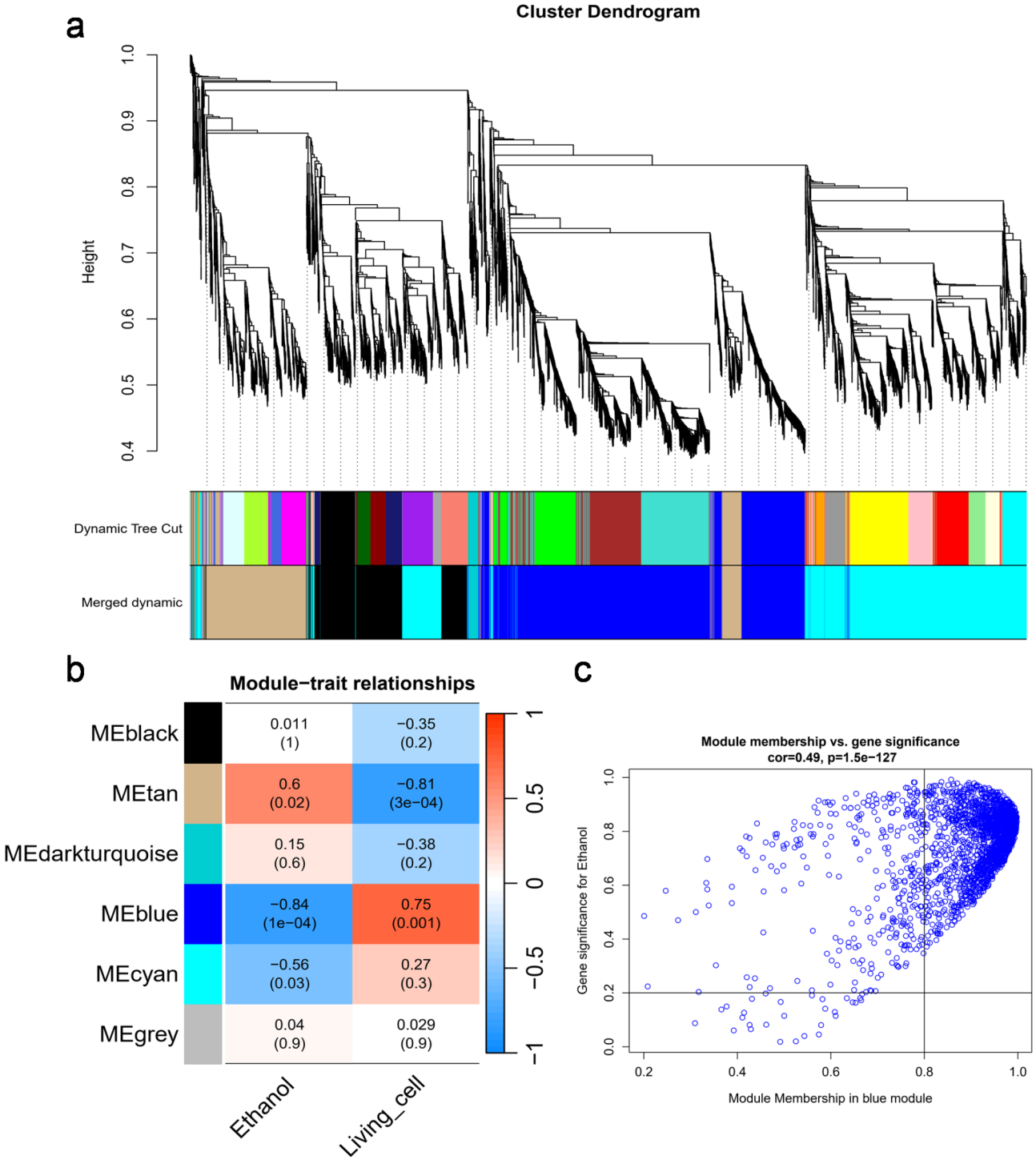

Fig. 2 Identification of key modules associated with the concerned traits. (**a**) Hierarchical cluster analysis was conducted to detect co-expression clusters with corresponding color assignments. Each branch in the clustering tree represents a gene, while each color represents a module in the constructed gene co-expression network by WGCNA. (**b**) Relationship of modules and traits. Each module contains the corresponding correlation coefficient (above) and *p*-value (below). (**c**) Scatterplot of Module membership (MM) vs. Gene significance (GS) for ethanol in the blue module. A total of 1756 genes meet the criteria of MM > 0.8 and GS > 0.2

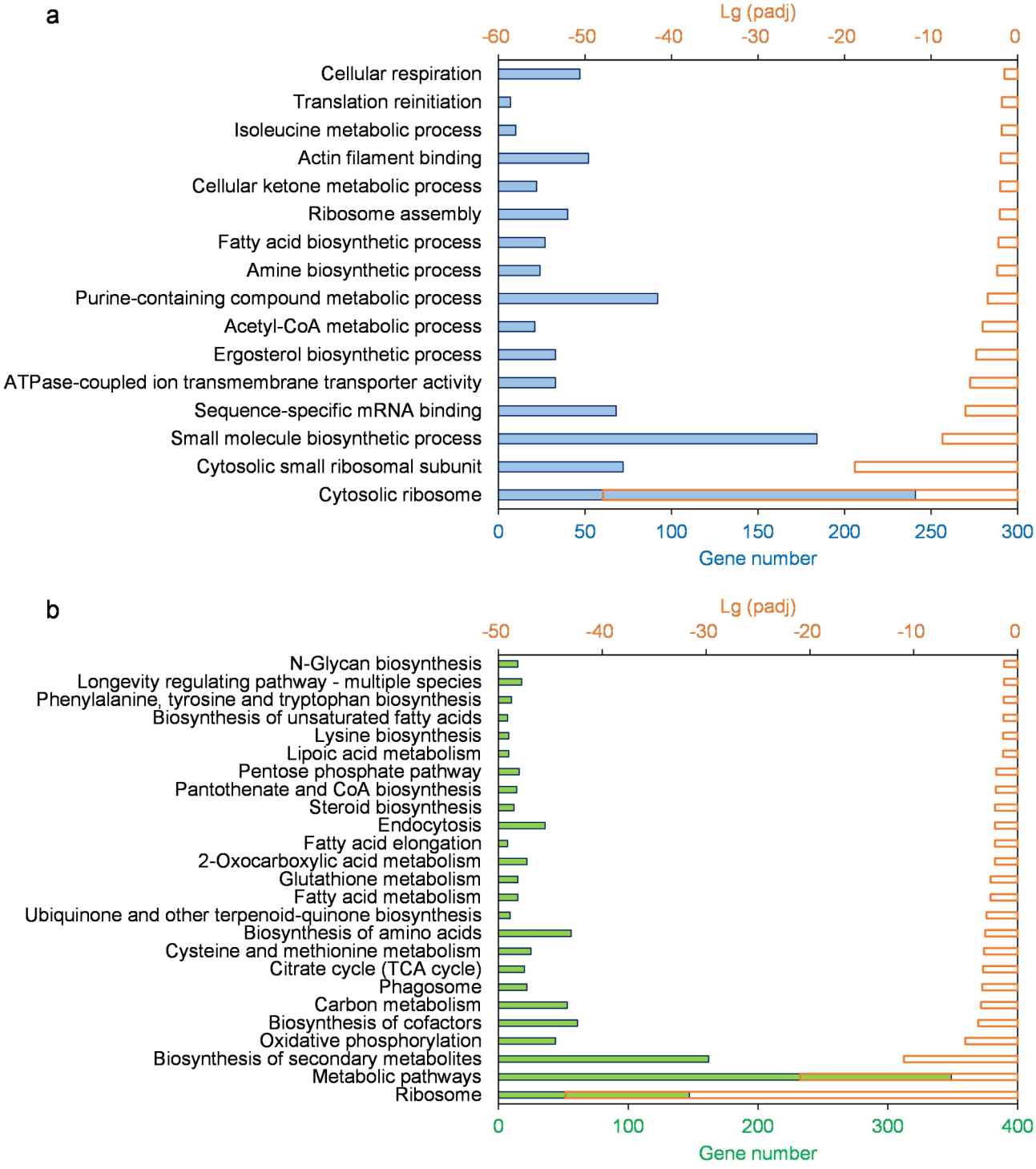

Fig. 3 Enriched GO terms (**a**) and KEGG pathways (**b**) for 1756 genes closely associated with ethanol (padj < 0.05)

for mitochondrial ribosome displayed a distinct expression pattern. Their expression levels increased from S1 to S2, and remained relatively high at S3 (Fig. S5). Mitochondrial ribosomes synthesize proteins encoded by the mitochondrial DNA. These proteins are primarily components of the oxidative phosphorylation complexes, which are essential for ATP production [24, 25]. The results suggested that cytoplasmic translation is profoundly affected by ethanol stress. However, the cells may preserve protein synthesis within the mitochondria to maintain vitality and ensure an adequate energy supply, thereby countering the effects of ethanol stress.

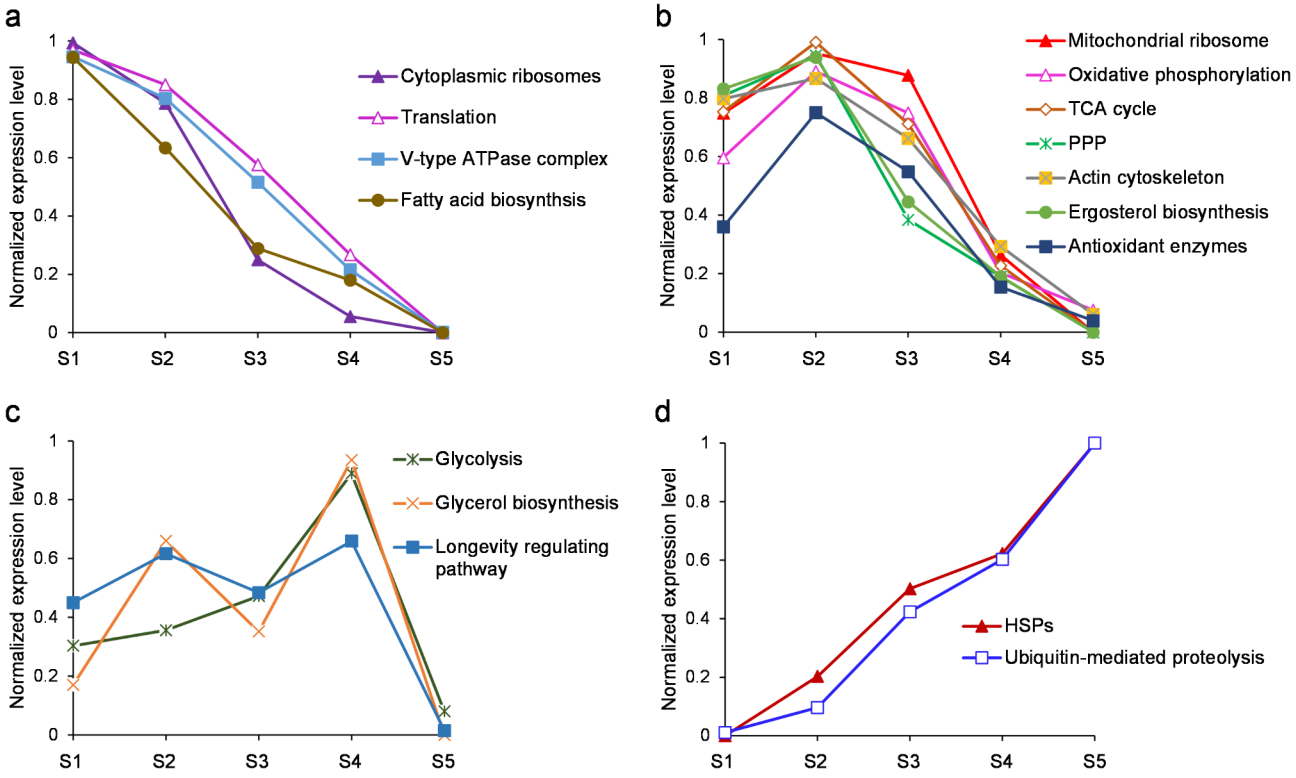

Fig. 4 Dynamic response of strain ES-42 to ethanol stress during continuous ethanol fermentation. The value of each point represents the average of the linearly normalized expression levels of all relevant genes. The expression levels of these genes reached their peaks at S1 (**a**), S2 (**b**), S4 (**c**), and S5 (**d**), respectively

Expression of genes associated with mitochondria

Cellular respiration and oxidative phosphorylation were significantly enriched in the GO and KEGG analyses, respectively. Genes encoding key enzymes for oxidative phosphorylation maintained high expression levels from S1 to S3, with a peak at S2 (Fig. S6a). Similarly, genes coding for mitochondrial enzymes essential for the TCA cycle, such as *LSC1*, *KGD1*, *KGD2*, and *ACO1*, also peaked at S2 but then decreased by more than 50% at S4 (Fig. 5). This suggested that the mitochondria were in a highly active state at S2, likely producing a greater amount of ATP to support cellular energy demands.

Expression of genes associated with central carbon metabolism

Given the profound connection between the fermentation process and central carbon metabolism, an exhaustive analysis of the central carbon metabolism is indispensable. The expression profiles of genes relevant to central carbon metabolism are illustrated in Fig. 5.

GO and KEGG enrichment analyses revealed significant enrichment in the PPP, acetyl-CoA synthesis, and TCA cycle (Fig. 3). Besides the TCA cycle, genes related to acetyl-CoA synthesis (*ALD4*, *ACS2*, *PDA1*, *PDB1*, *LAT1*) and the PPP (*SOL3*, *GND1*, *GND2*, *RPE1*, *RKI1*, *TKL1*) reached their highest expression levels at S2 (Fig. 5). Among these, *SOL3*, *GND1*, and *GND2* are responsible for NADPH production. The results suggested an increased synthesis of NADPH and acetyl-CoA at S2. In contrast, genes involved in glycolysis (*HXK2*, *GLK1*, *PFK1*, *PFK2*, *TDH2*, *GPM2*, *PGK3*, *ENO1*, *ENO2*, *CDC19*), glycerol biosynthesis (*GPD1*, *GPD2*, *GPP1*), and ethanol synthesis (*ADH1*, *ADH4*, *ADH5*) reached their highest levels at S4. Notably, glycerol synthesis genes *GPD1* and *GPP2* also showed relatively high expression at S2. Overall, throughout the fermentation process, genes related to the TCA cycle and synthesis of NADPH and acetyl-CoA showed higher expression at S1 and S2, while genes associated with glycolysis and synthesis of glycerol and ethanol reached their highest expression levels at S4. All gene expression levels declined to their lowest at S5.

Expression of genes associated with fatty acid and ergosterol biosynthesis

From S1 to S5, the expression levels of genes involved in the synthesis of very long-chain fatty acids (VLCFAs) gradually decreased (Fig. S6b). Meanwhile, the expression levels of genes involved in ergosterol synthesis increased from S1 to S2 but then dropped significantly thereafter (Fig. S6b). Fatty acids and ergosterol are crucial components of the cell membrane, helping to maintain its fluidity and stability [26, 27]. It has been reported that

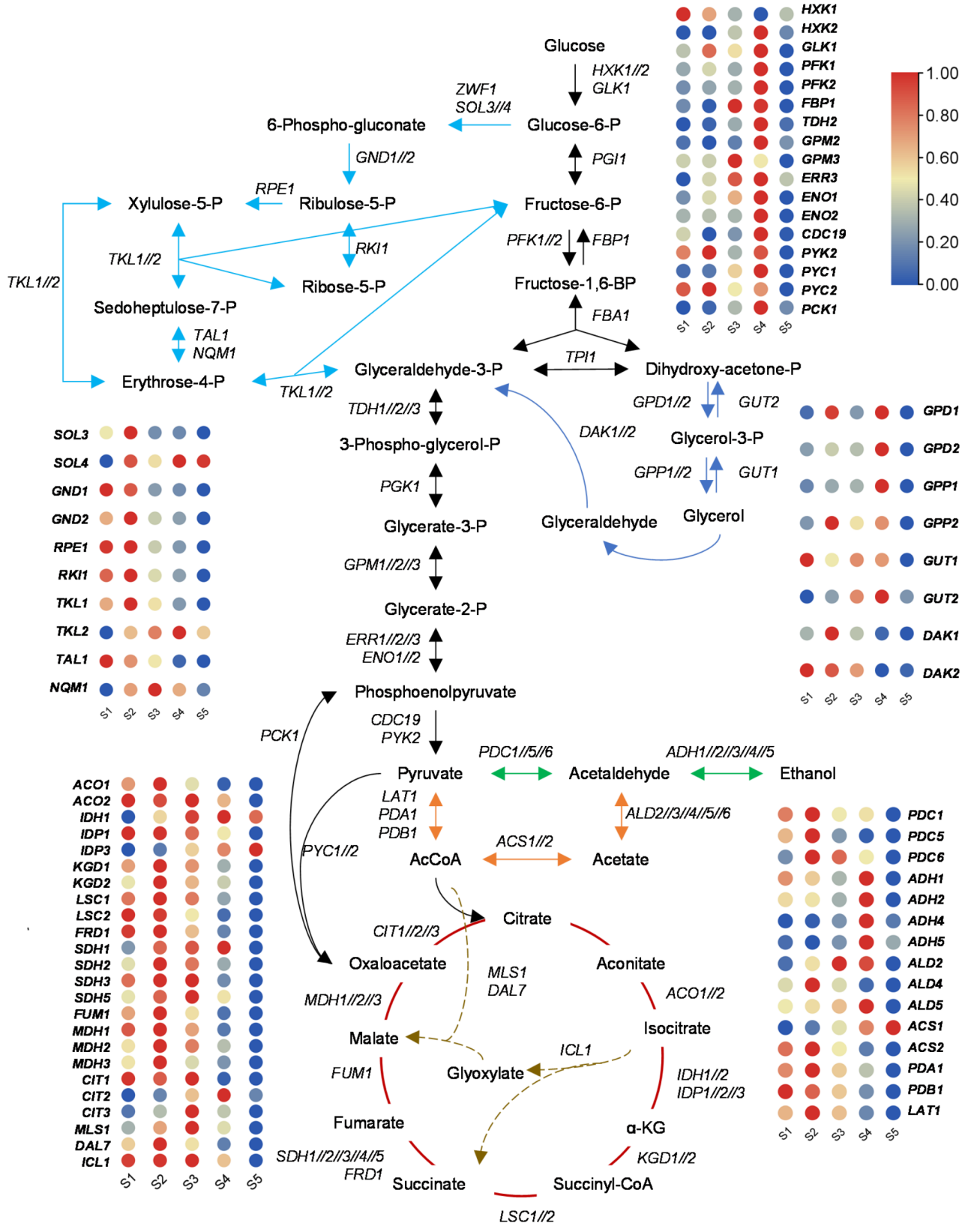

Fig. 5 Expression of genes related to central carbon metabolism during continuous ethanol fermentation. The data for each gene were linearly normalized based on the TPM values across different sampling points

maintaining high membrane fluidity and stability under ethanol stress can help cells combat the toxic effects of ethanol [28, 29]. However, their synthesis processes require substantial amounts of acetyl-CoA, ATP, and NADPH [30, 31], which can be detrimental to the cell's survival under ethanol stress. It is likely that yeast cells reduce the synthesis of fatty acids and ergosterol to avoid energy depletion, thereby helping cells overcome increasing ethanol stress.

Expression of genes associated with longevity regulatory pathway

The longevity regulatory pathway was significantly enriched. In yeast, lifespan and aging are modulated in response to nutrients via the TOR/Sch9 and Ras/PKA pathways [32, 33]. Both pathways ultimately rely on the serine-threonine kinase Rim15 and transcription factors (TFs) Gis1 and Msn2/4 to activate genes involved in antioxidant stress, energy metabolism, glucose metabolism, and HSPs protection [32, 33] (Fig. 6a).

In this study, the gene *CYR1*, which encodes adenylate cyclase and is essential for cAMP production, showed highest expression level at S2 and subsequently decreased as ethanol concentration increased (Fig. 6b). Genes encoding subunits of cAMP-dependent protein kinase (PKA), *TPK1* and *TPK2*, also exhibited a similar expression trend. These results suggested that Cyr1 and PKA may have the highest activity at S2 and the lowest at S5. Simultaneously, the expression levels of *MSN2*, *RIM15*, and *GIS1* gradually increased from S1 to S4. Notably, the expression trend of *MSN4* differed from that of *MSN2*, instead aligning with *TPK1* and *TPK2*.

Downstream genes regulated by these TFs also showed diverse expression trends. For instance, *SOD1*, *SOD2*, and *CTT1*, coding for antioxidant enzymes, reached their highest levels at S2, matching the expression trend of *MSN4*. Glycolysis genes had the highest expression levels at S4, consistent with the expression trend of *MSN2*, *RIM15*, and *GIS1*. Glycerol synthesis genes exhibited high expression levels at both S2 and S4, suggesting they might be regulated by these TFs in a dual manner. Additionally, genes related to HSPs and ubiquitin-mediated proteasomal degradation showed expression trends similar to those of *MSN2*, *RIM15*, and *GIS1* from S1 to S4, but reached their highest levels at S5. Overall, at S2, antioxidant enzyme and glycerol synthesis genes were activated; at S4, glycolysis, glycerol synthesis, HSPs, and protein degradation genes were activated. These changes are likely closely related to the longevity regulatory pathway. These findings suggested that the longevity regulatory pathway may play a crucial role in helping cells tolerate increasing ethanol stress.

In summary, the ethanol-tolerant *S. cerevisiae* strain ES-42 was found to cope with persistent ethanol stress through the regulation of energy metabolism, carbohydrate metabolism, and protein quality control (Fig. 7). Notably, cytoplasmic protein synthesis and fatty acid synthesis were suppressed to conserve ATP, while HSPs and ubiquitin-mediated proteolysis were activated to refold or degrade denatured proteins. These effects became more pronounced as the ethanol concentration

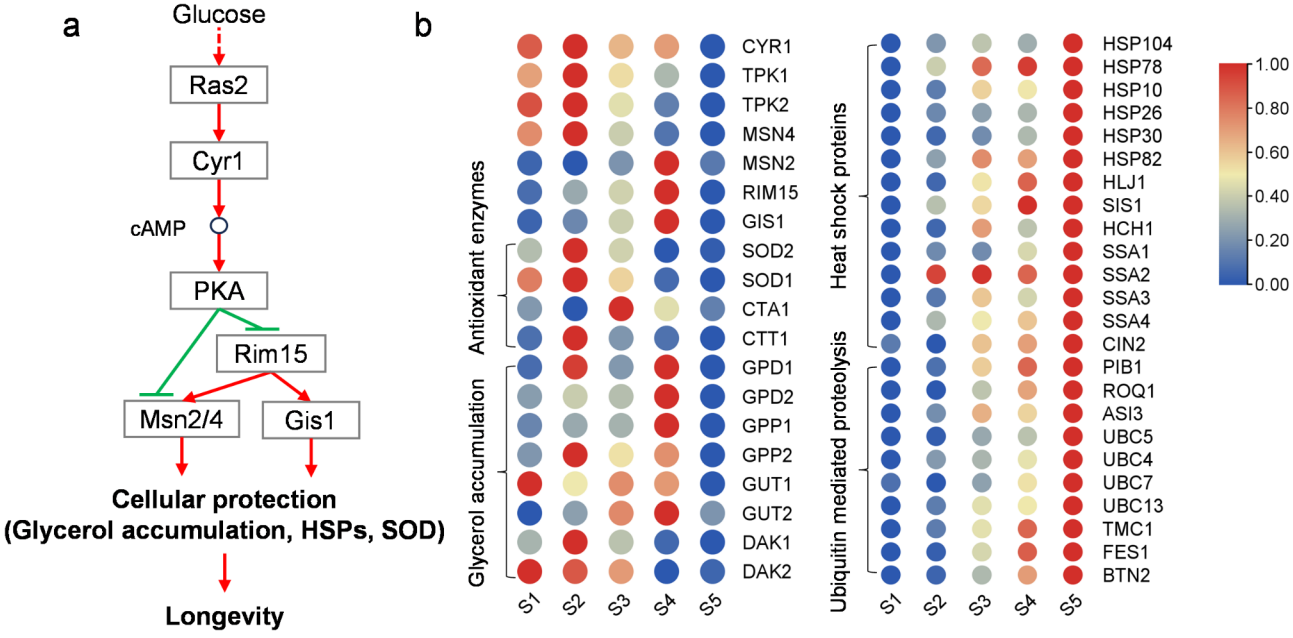

Fig. 6 (**a**) Longevity regulatory pathway. (**b**) Expression of genes associated with the longevity regulatory pathway. The data for each gene were linearly normalized based on the TPM values across different sampling points

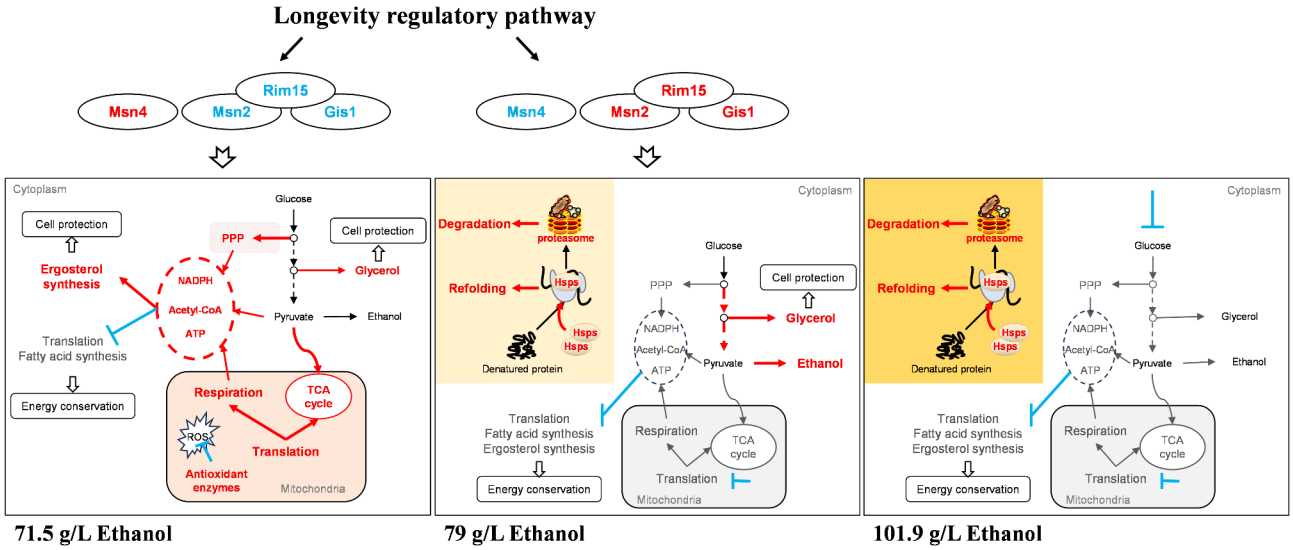

Fig. 7 Illustration of the response mechanisms of *S. cerevisiae* strains ES-42 to ethanol during continuous ethanol fermentation. The red color indicates upregulation, and the blue color indicates downregulation

increased. Beyond these general responses, distinct adaptations emerged at different ethanol concentrations. At approximately 71.5 g/L ethanol, cells activated the PPP, acetyl-CoA synthesis, and mitochondrial respiration to boost the production of NADPH, acetyl-CoA, and ATP, thereby supporting cell growth and metabolism. Concurrently, SOD and catalase were upregulated to counteract reactive oxygen species (ROS) generated during mitochondrial respiration. Additionally, the synthesis of ergosterol and glycerol was enhanced, contributing to greater ethanol resistance. At approximately 79 g/L ethanol, mitochondrial respiration, PPP, acetyl-CoA synthesis, and ergosterol synthesis were suppressed. In contrast, glycolysis, glycerol synthesis, and ethanol production were promoted. At an ethanol concentration of 86.9 g/L, the cellular response appeared to be an intermediate state between those observed at 71.5 g/L and 79 g/L, suggesting a gradual transition in metabolic strategies. These transitions in cellular responses across the range from 71.5 to 86.9 to 79 g/L ethanol may be regulated by the longevity regulating pathway. Finally, at an ethanol concentration of 101.9 g/L, all aforementioned activities were suppressed, and cells relied mainly on HSPs and protein degradation pathways to maintain protein homeostasis under extreme conditions.

Discussions

Currently, most studies have focused on the transcriptional changes in *S. cerevisiae* during short-term ethanol exposure [34–36]. However, these ethanol-induced responses may be transient, quickly returning to their original state after physiological adjustment. Investigating the transcriptional and regulatory mechanisms under long-term ethanol exposure is of great importance and urgency.

We compared our results with a previous study on the transcriptional profiles of yeast during continuous ethanol fermentation [15]. They also found repressed ergosterol synthesis and upregulated unfolded protein responses. The repression of ergosterol synthesis was attributed to the synergistic effect of ethanol and hypoxia in multistage fermenters. In the present study, genes related to ergosterol synthesis were upregulated at S2 but downregulated at S3-S5 compared to S1. Ergosterol helps maintain membrane stability and plays a role in ethanol tolerance [26, 37]. It is speculated that cells may enhance ergosterol synthesis at S2 to resist ethanol stress. After S2, the repression of ergosterol synthesis may be partly due to high ethanol concentration. Since ergosterol synthesis requires significant amounts of ATP, acetyl-CoA, and NADPH [30, 31], limited precursors or energy conservation could be reasons for the inhibition of synthesis.

Protein denaturation was observed both in long-term and short-term exposure to ethanol stress [15, 38]. The unfolded protein response (UPR) signals the accumulation of misfolded proteins and activates HSPs and ubiquitin-mediated degradation to clear the misfolded proteins [39]. In the present study, genes related to HSPs and ubiquitin-mediated degradation were consistently upregulated, likely helping cells clear the ethanol-induced denatured proteins. Therefore, we speculate that the rapid degradation of denatured proteins may be a necessary condition for yeast cells to possess excellent ethanol tolerance.

Transcriptional changes in genes associated with mitochondrial ribosomes, observed in the present study, have not been previously reported. Specifically, compared to

S1, genes associated with mitochondrial ribosomes were upregulated at S2, concurrent with the activation of oxidative phosphorylation. Mitochondrial ribosomes are responsible for translating mitochondrial DNA, which predominantly encodes components of oxidative phosphorylation complexes [25]. This result suggested that cells may enhance mitochondrial function to ensure an adequate energy supply under ethanol stress. However, as the ethanol concentration increased, mitochondrial function was progressively inhibited. This phenomenon could be attributed to the fact that, while respiration produces ATP, it also produces ROS in the electron transport chain, which can damage cellular components [40]. Reducing respiration might therefore be beneficial to limit such damage.

One interesting finding is that the lifespan regulation pathway may play a protective role in cells under continuous ethanol stress. The lifespan and aging of yeast cells are controlled by the Ras-PKA signaling pathway and its downstream TFs, Msn2/4, and Gis1 [32, 33]. Besides regulating genes related to general stress response and HSPs, the lifespan regulation pathway also controls the metabolic shift from the TCA cycle and respiration to glycolysis and glycerol synthesis to extend lifespan [33]. The role of glycerol synthesis in lifespan regulation includes providing nutritional support for long-term cell survival, enhancing resistance to osmotic stress, and regulating redox homeostasis [33, 41]. In this study, glycerol synthesis genes showed similar expression trends to those involved in the lifespan regulation pathway, exhibiting bimodal expression at S2 and S4 (Fig. 4). This suggested that the lifespan regulation pathway may partly enhance cellular tolerance to ethanol stress by regulating glycerol synthesis. Currently, the role of the lifespan regulation pathway in ethanol tolerance is unclear, and further investigation in this regard is warranted.

Finally, to develop an *S. cerevisiae* strain with enhanced ethanol tolerance, several key TFs within the longevity-regulating pathway may serve as promising engineering targets. Under low ethanol stress, deleting *MSN2*, *RIM15*, and *GIS1* and overexpressing *MSN4* might enhance ethanol tolerance by activating mitochondrial respiration and promoting the synthesis of antioxidant enzymes and glycerol. Conversely, under high ethanol stress, overexpressing *MSN2*, *RIM15*, and *GIS1* might induce a metabolic shift from respiration towards glycerol production and enhance the cellular capacity for clearing denatured proteins. These targets provide a foundation for developing genetic engineering strategies to improve yeast strain performance under ethanol stress.

Conclusion

This study conducted a 61-day one-stage continuous ethanol fermentation and elucidated the response mechanisms of the ethanol-tolerant *S. cerevisiae* strain ES-42 to increasing ethanol concentrations through comparative transcriptomics analysis. Based on these findings, we proposed potential mechanisms by which yeast cells tolerated increasing ethanol concentrations. Under low ethanol stress, cells activated respiration to supply energy and enhanced the synthesis of NADPH, acetyl-CoA, ergosterol, and glycerol to resist stress. Under relatively high ethanol stress, cells inhibited respiration, increased glycerol synthesis, and promoted the refolding and degradation of denatured proteins to protect cells. As ethanol concentration increased, the ability to clear denatured proteins became progressively more critical for maintaining cellular function and viability. The longevity-regulating pathway likely played a crucial role in mediating the transition between these different response mechanisms as ethanol concentrations rose. This study provides a deeper insight into the dynamic response mechanisms of ethanol-tolerant yeast cells during continuous ethanol fermentation, offering valuable information for engineering strains with enhanced ethanol tolerance.

Abbreviations

ARTP	Atmospheric and room temperature plasma
ATP	Adenosine-triphosphate
ER	Endoplasmic reticulum
FID	Flame ionization detector
GC	Gas chromatography
GO	Gene Ontology
GS	Gene significance
HPLC	High-performance liquid chromatography
HSPs	Heat shock proteins
KEGG	Kyoto Encyclopedia of Genes and Genomes
MM	Module membership
NADPH	Nicotinamide adenine dinucleotide phosphate
PCA	Principal component analysis
PKA	Protein kinase
PPP	Pentose phosphate pathway
RNA	Ribonucleic Acid
ROS	Reactive oxygen species
S. cerevisiae	*Saccharomyces cerevisiae*
TCA cycle	Tricarboxylic acid cycle
TFs	Transcription factors
TOM	Topological overlap matrix
TPM	Transcripts per million reads
UPR	Unfolded protein response
VHG	Very high gravity
VLCFAs	Very long-chain fatty acids
WGCNA	Weighted gene co-expression network analysis

Supplementary Information

The online version contains supplementary material available at https://doi.org/10.1186/s12934-025-02663-7.

Supplementary Material 1

Supplementary Material 2

Acknowledgements
Not applicable.

Author contributions
XX J, BX Y, and QR S conducted experiments. XX J and CY X analyzed data and wrote the main manuscript. Q Z and ZY S provided technical assistance during the experiment and data analysis. YQ T designed the study, revised the manuscript, and acquired financial support. All authors read and approved of the final manuscript.

Funding
This study was financially supported by the National Key R&D Program of China (2022YFE0108500) and the National Natural Science Foundation of China (52300169).

Data availability
The dataset(s) used and/or analyzed during the current study are available from the corresponding author on reasonable request. The raw sequence data can be accessed in the National Center for Biotechnology Information (http://www.ncbi.nlm.nih.gov/) through SRA accession number PRJNA1114950.

Declarations

Ethics approval and consent to participate
Not applicable.

Consent for publication
Not applicable.

Competing interests
The authors declare no competing interests.

Author details
[1]College of Architecture and Environment, Sichuan University, Chengdu 610065, Sichuan, China
[2]Sichuan Environmental Protection Key Laboratory of Organic Wastes Valorization, Chengdu 610065, Sichuan, China
[3]Sinopec (Dalian) Research Institute of Petroleum and Petrochemicals Co. Ltd, Dalian, Liaoning 115045, China
[4]Engineering Research Center of Alternative Energy Materials & Devices, Ministry of Education, Chengdu 610065, Sichuan, China

Received: 25 November 2024 / Accepted: 24 January 2025
Published online: 30 January 2025

References

1. Bai FW, Anderson WA, Moo-Young M. Ethanol fermentation technologies from sugar and starch feedstocks. Biotechnol Adv. 2008;26:89–105.
2. Mohd Azhar SH, Abdulla R, Jambo SA, Marbawi H, Gansau JA, Mohd Faik AA, et al. Yeasts in sustainable bioethanol production: a review. Biochem Biophys Rep. 2017;10:52–61.
3. Stanley D, Bandara A, Fraser S, Chambers PJ, Stanley GA. The ethanol stress response and ethanol tolerance of *Saccharomyces cerevisiae*. J Appl Microbiol. 2010;109:13–24.
4. Shen Y, Zhao XQ, Ge XM, Bai FW. Metabolic flux and cell cycle analysis indicating new mechanism underlying process oscillation in continuous ethanol fermentation with *Saccharomyces cerevisiae* under VHG conditions. Biotechnol Adv. 2009;27:1118–23.
5. Bayrock DP, Michael Ingledew W. Application of multistage continuous fermentation for production of fuel alcohol by very-high-gravity fermentation technology. J Ind Microbiol Biotechnol. 2001;27:87–93.
6. Bai FW, Chen LJ, Anderson WA, Moo-Young M. Parameter oscillations in a very high gravity medium continuous ethanol fermentation and their attenuation on a multistage packed column bioreactor system. Biotechnol Bioeng. 2004;88:558–66.
7. Thani A, Lin YH, Laopaiboon P, Laopaiboon L. Variation of fermentation redox potential during cell-recycling continuous ethanol operation. J Biotechnol. 2016;239:68–75.
8. Liang C, Ding S, Sun W, Liu L, Zhao W, Zhang D, et al. Biofilm-based fermentation: a novel immobilisation strategy for *Saccharomyces cerevisiae* cell cycle progression during ethanol production. Appl Microbiol Biotechnol. 2020;104:7495–505.
9. Jhariya U, Dafale NA, Srivastava S, Bhende RS, Kapley A, Purohit HJ. Understanding ethanol tolerance mechanism in to enhance the bioethanol production: current and future prospects. Bioenerg Res. 2021;14:670–88.
10. Aguilera F, Peinado RA, Millán C, Ortega JM, Mauricio JC. Relationship between ethanol tolerance, H-ATPase activity and the lipid composition of the plasma membrane in different wine yeast strains. Int J Food Microbiol. 2006;110:34–42.
11. Kubota S, Takeo I, Kume K, Kanai M, Shitamukai A, Mizunuma M, et al. Effect of ethanol on cell growth of budding yeast: genes that are important for cell growth in the presence of ethanol. Biosci Biotechnol Biochem. 2004;68:968–72.
12. Cray JA, Stevenson A, Ball P, Bankar SB, Eleutherio ECA, Ezeji TC, et al. Chaotropicity: a key factor in product tolerance of biofuel-producing microorganisms. Curr Opin Biotechnol. 2015;33:228–59.
13. Ma MG, Liu ZL. Mechanisms of ethanol tolerance in *Saccharomyces cerevisiae*. Appl Microbiol Biotechnol. 2010;87:829–45.
14. Snoek T, Verstrepen KJ, Voordeckers K. How do yeast cells become tolerant to high ethanol concentrations? Curr Genet. 2016;62:475–80.
15. Li BZ, Cheng JS, Qiao B, Yuan YJ. Genome-wide transcriptional analysis of *Saccharomyces cerevisiae* during industrial bioethanol fermentation. J Ind Microbiol Biotechnol. 2010;37:43–55.
16. Zhang X, Wang L, Li Q, den Haan R, Li F, Liu CG, et al. Omics analysis reveals mechanism underlying metabolic oscillation during continuous very-high-gravity ethanol fermentation by *Saccharomyces cerevisiae*. Biotechnol Bioeng. 2021;118:2990–3001.
17. Wang L, Li B, Wang SP, Xia ZY, Gou M, Tang YQ. Improving multiple stress-tolerance of a flocculating industrial *Saccharomyces cerevisiae* strain by random mutagenesis and hybridization. Process Biochem. 2021;102:275–85.
18. Thani A, Laopaiboon P, Laopaiboon L. Improvement of a continuous ethanol fermentation from sweet sorghum stem juice using a cell recycling system. J Biotechnol. 2017;251:21–9.
19. Hernandez-Cortes G, Valle-Rodriguez JO, Herrera-Lopez EJ, Diaz-Montano DM, Gonzalez-Garcia Y, Escalona-Buendia HB, et al. Improvement on the productivity of continuous tequila fermentation by *Saccharomyces cerevisiae* of Agave tequilana juice with supplementation of yeast extract and aeration. AMB Express. 2016;6:47.
20. Wu YJ, Li B, Miao B, Xie CY, Tang YQ. *Saccharomyces cerevisiae* employs complex regulation strategies to tolerate low pH stress during ethanol production. Microb Cell Fact. 2022;21:247.
21. Langfelder P, Horvath S. WGCNA: an R package for weighted correlation network analysis. BMC Bioinformatics. 2008;9:559.
22. Gao XM, Zhou XH, Jia MW, Wang XZ, Liu D. Identification of key genes in sepsis by WGCNA. Prev Med. 2023;172:107540.
23. Zhou Y, Zhou B, Pache L, Chang M, Khodabakhshi AH, Tanaseichuk O, et al. Metascape provides a biologist-oriented resource for the analysis of systems-level datasets. Nat Commun. 2019;10:1523.
24. Lopez Sanchez MIG, Kruger A, Shiriaev DI, Liu Y, Rorbach J. Human mitoribosome biogenesis and its emerging links to disease. Int J Mol Sci. 2021;22.
25. Harper NJ, Burnside C, Klinge S. Principles of mitoribosomal small subunit assembly in eukaryotes. Nature. 2023;614:175–81.
26. Henderson CM, Block DE. Examining the role of membrane lipid composition in determining the ethanol tolerance of *Saccharomyces cerevisiae*. Appl Environ Microbiol. 2014;80:2966–72.
27. Ballweg S, Ernst R. Control of membrane fluidity: the OLE pathway in focus. Biol Chem. 2017;398:215–28.
28. Yang YJ, Xia YJ, Hu WY, Tao LR, Ni L, Yu JS et al. Membrane fluidity of *Saccharomyces cerevisiae* from *Huangjiu* (Chinese rice wine) is variably regulated by *OLE1* to offset the disruptive effect of ethanol. Appl Environ Microbiol. 2019;85.
29. Kim HS, Kim NR, Choi W. Total fatty acid content of the plasma membrane of *Saccharomyces cerevisiae* is more responsible for ethanol tolerance than the degree of unsaturation. Biotechnol Lett. 2011;33:509–15.
30. Hu ZH, He B, Ma L, Sun YL, Niu YL, Zeng B. Recent advances in ergosterol biosynthesis and regulation mechanisms in *Saccharomyces cerevisiae*. Indian J Microbiol. 2017;57:270–7.
31. Gossing M, Smialowska A, Nielsen J. Impact of forced fatty acid synthesis on metabolism and physiology of *Saccharomyces cerevisiae*. FEMS Yeast Res. 2018;18.

32. Mirisola MG, Longo VD. Yeast chronological lifespan: longevity regulatory genes and mechanisms. Cells. 2022;11.
33. Wei M, Fabrizio P, Madia F, Hu J, Ge H, Li LM, et al. Tor1/Sch9-regulated carbon source substitution is as effective as calorie restriction in life span extension. PLoS Genet. 2009;5:e1000467.
34. Li R, Xiong G, Yuan S, Wu Z, Miao Y, Weng P. Investigating the underlying mechanism of *Saccharomyces cerevisiae* in response to ethanol stress employing RNA-seq analysis. World J Microbiol Biotechnol. 2017;33:206.
35. Li R, Miao Y, Yuan S, Li Y, Wu Z, Weng P. Integrated transcriptomic and proteomic analysis of the ethanol stress response in *Saccharomyces cerevisiae* Sc131. J Proteom. 2019;203:103377.
36. Ando R, Ishikawa Y, Kamada Y, Izawa S. Contribution of the yeast bi-chaperone system in the restoration of the RNA helicase Ded1 and translational activity under severe ethanol stress. J Biol Chem. 2023;299.
37. Vanegas JM, Contreras MF, Faller R, Longo ML. Role of unsaturated lipid and ergosterol in ethanol tolerance of model yeast biomembranes. Biophys J. 2012;102:507–16.
38. Kato S, Yoshida M, Izawa S. Btn2 is involved in the clearance of denatured proteins caused by severe ethanol stress in *Saccharomyces cerevisiae*. FEMS Yeast Res. 2019;19.
39. Hartl FU, Bracher A, Hayer-Hartl M. Molecular chaperones in protein folding and proteostasis. Nature. 2011;475:324–32.
40. Orlandi I, Ronzulli R, Casatta N, Vai M. Ethanol and acetate acting as carbon/energy sources negatively affect yeast chronological aging. Oxid Med Cell Longev. 2013;2013:802870.
41. Blomberg A. Yeast osmoregulation - glycerol still in pole position. FEMS Yeast Res. 2022;22.

Publisher's note